

Effect of anisotropic in-plane strains on phase states and dielectric properties of epitaxial ferroelectric thin films

A. G. Zembilgotov,^{a)} N. A. Pertsev,^{b)} U. Böttger, and R. Waser^{c)}

*Institut für Werkstoffe der Elektrotechnik, RWTH Aachen University of Technology,
D-52056 Aachen, Germany*

(Received 6 August 2004; accepted 29 November 2004; published online 28 January 2005)

A nonlinear thermodynamic theory is used to predict the equilibrium polarization states and dielectric properties of ferroelectric thin films grown on dissimilar substrates which induce anisotropic strains in the film plane. The “misfit strain-temperature” phase diagrams are constructed for single-domain PbTiO_3 and $\text{Pb}_{0.35}\text{Sr}_{0.65}\text{TiO}_3$ films on orthorhombic substrates. It is shown that the in-plane strain anisotropy may lead to the appearance of new phases which do not form in films grown on cubic substrates. The strain-induced dielectric anisotropy in the film plane is also calculated and compared with the anisotropy observed in $\text{Pb}_{0.35}\text{Sr}_{0.65}\text{TiO}_3$ films deposited on NdGaO_3 . © 2005 American Institute of Physics. [DOI: 10.1063/1.1855389]

Physical properties of single-crystal ferroelectric films are intensively studied experimentally^{1–6} and theoretically.^{7–13} Up to now, the theoretical investigations were restricted to thin films grown on (001)-oriented cubic substrates. In this particular case, the strain field is isotropic in the film plane. However, other substrates (e.g., orthorhombic) generally will induce the in-plane strain anisotropy. Recent experiments have shown that the strain anisotropy may significantly affect the film dielectric properties.¹⁴ In this letter, we extend the thermodynamic theory of ferroelectric thin films^{7,11} to epitaxial layers with anisotropic in-plane strains.

We shall consider single-domain ferroelectric films grown in the (001)-oriented cubic paraelectric phase on a dissimilar substrate. In general, the substrate induces two different in-plane strains, u_1 and u_2 , and a shear deformation u_6 in the film. (We use the Voigt matrix notation and the reference frame with the x_3 axis orthogonal to the film surfaces.) The strain field inside the film is taken to be homogeneous in our theory. (This approximation can be used even for films containing a thin inhomogeneously strained layer near the interface, being caused, e.g., by the presence of misfit dislocations¹⁵ or a superstructure.¹⁶) Since the in-plane strains are governed by a thick substrate, they can be regarded as fixed parameters of the film/substrate system: $u_1 = u_{m1}$, $u_2 = u_{m2}$, $u_6 = u_{m6}$. The misfit strains can be calculated as $u_{m1} = (a_1 - a_0)/a_0$, $u_{m2} = (a_2 - a_0)/a_0$, and $u_{m6} = \gamma - \pi/2$, where a_0 is the equivalent cubic cell constant of the free-standing film, a_1 and a_2 are the in-plane lattice constants of the epitaxial film, and γ is the angle between (100) and (010) crystallographic axes in the strained film.¹⁷

For epitaxial films with a mechanically free upper surface, the equilibrium thermodynamic states can be found via the minimization of a modified thermodynamic potential \tilde{G} ,⁷ which is derived by the Legendre transformation of the standard elastic Gibbs function G .¹⁸ Performing necessary calcu-

lations, we obtained the following generalized expression for the modified potential \tilde{G} as a function of the polarization components P_i ($i = 1, 2, 3$):

$$\begin{aligned} \tilde{G} = & \alpha_1^* P_1^2 + \alpha_2^* P_2^2 + \alpha_3^* P_3^2 + \alpha_6^* P_1 P_2 + \alpha_{11}^* (P_1^4 + P_2^4) \\ & + \alpha_{33}^* P_3^4 + \alpha_{13}^* (P_1^2 + P_2^2) P_3^2 + \alpha_{12}^* P_1^2 P_2^2 + \alpha_{111}^* (P_1^6 + P_2^6 \\ & + P_3^6) + \alpha_{112}^* [P_1^4 (P_2^2 + P_3^2) + P_2^4 (P_1^2 + P_3^2) + P_3^4 (P_1^2 + P_2^2)] \\ & + \alpha_{123}^* P_1^2 P_2^2 P_3^2 + \frac{[s_{11}(u_{m1}^2 + u_{m2}^2) - 2s_{12}u_{m1}u_{m2}]}{2(s_{11}^2 - s_{12}^2)} + \frac{u_{m6}^2}{2s_{44}}, \end{aligned} \quad (1)$$

where

$$\begin{aligned} \alpha_1^* = & \alpha_1 + \frac{u_{m1}(Q_{12}s_{12} - Q_{11}s_{11}) + u_{m2}(Q_{11}s_{12} - Q_{12}s_{11})}{(s_{11}^2 - s_{12}^2)}, \\ \alpha_2^* = & \alpha_1 + \frac{u_{m2}(Q_{12}s_{12} - Q_{11}s_{11}) + u_{m1}(Q_{11}s_{12} - Q_{12}s_{11})}{(s_{11}^2 - s_{12}^2)}, \\ \alpha_3^* = & \alpha_1 - \frac{Q_{12}(u_{m1} + u_{m2})}{(s_{11} + s_{12})}, \quad \alpha_6^* = -\frac{Q_{44}}{s_{44}}u_{m6}, \end{aligned}$$

where α_1 , α_{ij} , and α_{ijk} are the dielectric stiffness coefficients at constant stress, s_{ln} are the elastic compliances at constant polarization, Q_{ln} are the electrostrictive constants, and α_{ij}^* are the renormalized coefficients introduced in Ref. 7. Equation (1) shows that the anisotropy of normal strains affects only the second-order polarization terms $\alpha_1^* P_1^2$ and $\alpha_2^* P_2^2$. On the other hand, in the presence of a nonzero shear strain u_{m6} , the film energy becomes dependent on the sign of polarization components P_1 and P_2 .

Using the derived potential \tilde{G} , we calculated the “misfit strain-temperature” phase diagram of PbTiO_3 (PT) films grown on (001)-oriented orthorhombic substrates.¹⁹ For the material parameters of PT involved in Eq. (1), we employed the numerical values listed in Ref. 7. In the discussed case, $u_{m6} = 0$ so that the phase diagram can be constructed using the misfit strains u_{m1} , u_{m2} , and temperature T as three independent variables. The cross section of the developed 3D diagram by the plane $u_{m1} = -u_{m2}$ is shown in the Fig. 1. This

^{a)}Permanent address: State Polytechnical University, 195251 St. Petersburg, Russia.

^{b)}Permanent address: A. F. Ioffe Physico-Technical Institute, Russian Academy of Sciences, 194021 St. Petersburg, Russia; electronic mail: pertsev@domain.ioffe.rssi.ru

^{c)}Also at Institut für Festkörperforschung, Forschungszentrum Jülich, D-52425 Jülich, Germany.

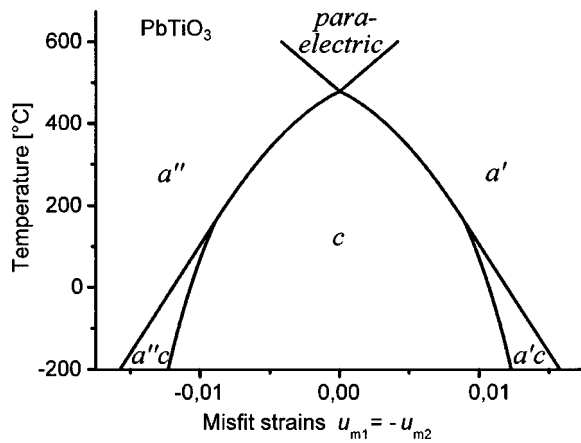


FIG. 1. Vertical cross section of the 3D phase diagram of PbTiO_3 thin films grown on dissimilar orthorhombic substrates. This cross section corresponds to the plane $u_{m1} = -u_{m2}$ and contains stability ranges of the following polarization states: c phase with the spontaneous polarization \mathbf{P}_s orthogonal to the interface; a' and a'' states, where \mathbf{P}_s is oriented along the $[100]$ and $[010]$ crystallographic axes, respectively; ca' and ca'' states with \mathbf{P}_s inclined to the interface and parallel to the (010) or (100) plane. The first- and second-order phase transitions are shown by thick and thin lines, respectively.

phase map is very different from the diagram of PT films grown on cubic substrates.⁷ (The latter represents the cross section of 3D diagram by the plane $u_{m1} = u_{m2}$.) Remarkably, when the misfit strains are opposite in sign, new ferroelectric phases appear, which do not form at $u_{m1} = u_{m2}$. These are the a phase, where the spontaneous polarization \mathbf{P}_s is oriented along one of the in-plane edges of the prototypic unit cell, and the ca phase, where \mathbf{P}_s is parallel to one of the out-of-plane faces of this cell.

The phase map of PT films at room temperature is shown in Fig. 2. It should be emphasized that anisotropic misfit strains ($u_{m1} \neq u_{m2}$) lower the symmetry of the paraelectric phase from cubic to orthorhombic. Hence, the symmetry of ferroelectric phases also lowers. Instead of the monoclinic r phase ($P_1 = P_2 \neq 0, P_3 \neq 0$) forming in PT films grown on cubic substrates,⁷ the triclinic r^* phase ($P_1 \neq P_2 \neq P_3 \neq 0$) appears in the general case. The strain anisotropy also transforms the aa phase ($|P_1| = |P_2| \neq 0, P_3 = 0$) into the aa^* phase, where \mathbf{P}_s is rotated away from the in-plane face diagonal of the unit cell ($P_1 \neq P_2 \neq 0, P_3 = 0$).

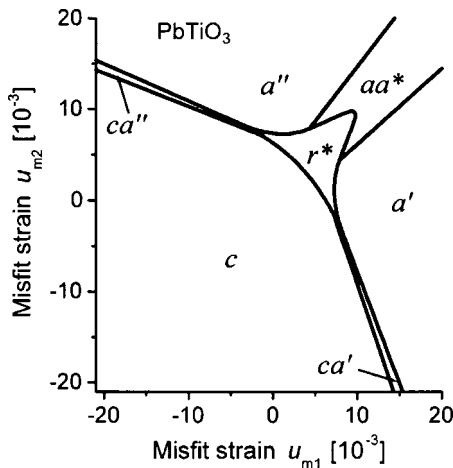


FIG. 2. Horizontal cross section of the 3D phase diagram of single-domain PbTiO_3 films grown on dissimilar orthorhombic substrates. The phase map corresponds to $T = 25^\circ\text{C}$.

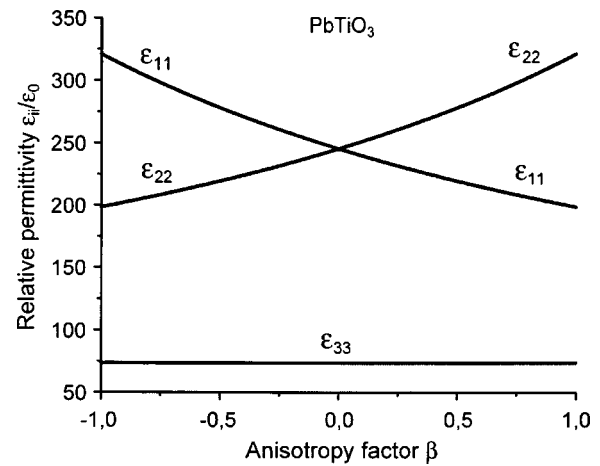


FIG. 3. Effect of the in-plane strain anisotropy on the dielectric constants of epitaxial PbTiO_3 films ($T = 25^\circ\text{C}$). The anisotropy factor equals $\beta = (u_{m1} - u_{m2}) / (u_{m1} + u_{m2})$. The dependencies are calculated at $u_{m1} + u_{m2} = -10 \times 10^{-3}$; they are valid only within the stability range of the c phase.

Since the renormalized second-order coefficients α_{ij}^* of PT films are positive,⁷ the paraelectric to ferroelectric phase transition is of the second order. The temperature T_c of this transition can be calculated analytically as $T_c = \max\{T_1, T_2, T_3\}$, where

$$T_1 = T_0 + \varepsilon_0 C \left(\frac{Q_{11} + Q_{12}}{s_{11} + s_{12}} (u_{m1} + u_{m2}) + \frac{Q_{11} - Q_{12}}{s_{11} - s_{12}} (u_{m1} - u_{m2}) \right)$$

$$T_2 = T_0 + \varepsilon_0 C \left(\frac{Q_{11} + Q_{12}}{s_{11} + s_{12}} (u_{m1} + u_{m2}) - \frac{Q_{11} - Q_{12}}{s_{11} - s_{12}} (u_{m1} - u_{m2}) \right)$$

$$T_3 = T_0 + 2\varepsilon_0 C \frac{Q_{12}(u_{m1} + u_{m2})}{(s_{11} + s_{12})}, \quad (2)$$

T_0 and C are the Curie–Weiss temperature and constant of a bulk crystal, and ε_0 is the permittivity of the vacuum. Equation (2) demonstrates that the anisotropy of *positive* misfit strains always raises T_c , whereas the anisotropy of *negative* misfit strains does not affect this temperature.

The dielectric properties of ferroelectric films must depend on the strain anisotropy as well. To demonstrate this effect, we calculated small-signal dielectric constants ε_{ij} of PT films with the out-of-plane polarization state ($P_1 = P_2 = 0, P_3 \neq 0$). When $u_{m1} = u_{m2}$, this state corresponds to the tetragonal c phase so that the dielectric response is isotropic in the film plane. At $u_{m1} \neq u_{m2}$, the symmetry of the c phase lowers to orthorhombic, which induces the in-plane dielectric anisotropy ($\varepsilon_{11} \neq \varepsilon_{22}$). Variations of the film dielectric constants with the anisotropy factor $\beta = (u_{m1} - u_{m2}) / (u_{m1} + u_{m2})$ are shown in Fig. 3. It can be seen that the strain-induced anisotropy of the in-plane dielectric response may be significant.

In order to compare our theoretical predictions with available experimental data,¹⁴ we also calculated the equilibrium phase states and dielectric properties of $\text{Pb}_{0.35}\text{Sr}_{0.65}\text{TiO}_3$ (PST) films grown on orthorhombic substrates. For PST of

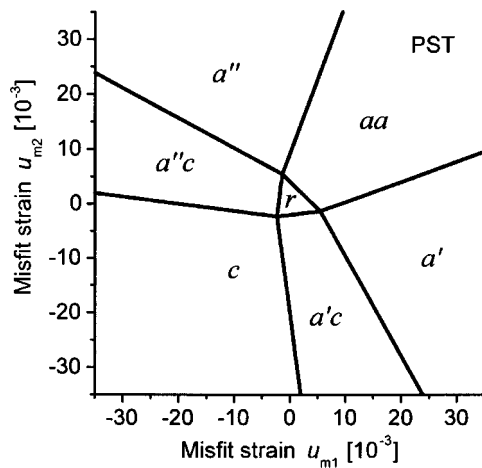


FIG. 4. Phase map of single-domain $\text{Pb}_{0.35}\text{Sr}_{0.65}\text{TiO}_3$ films grown on dissimilar orthorhombic substrates. The temperature is taken to be 25 °C.

this composition, we determined the dielectric stiffness $\alpha_1 = (T - T_0)/(2\epsilon_0 C)$ from the experimental values of T_0 and C .²⁰ Other material parameters of PST were calculated as weighted averages of those known for pure PbTiO_3 and SrTiO_3 .^{7,21} The developed phase diagram of PST films at room temperature is shown in Fig. 4. Evidently, it differs from the diagram of PT films (see Fig. 2). In particular, at very small misfit strains, the 2D clamping stabilizes the r^* phase in PST films, but not the c phase as in PT films. Since all three polarization components differ from zero in the r^* phase, the physical properties of a clamped PST film are expected to deviate markedly from those of a mechanically free PST, which stabilizes in the tetragonal ferroelectric phase.²²

The constructed diagram was used to evaluate the in-plane permittivities of the PST film grown on (110)-oriented NdGaO_3 substrate. The misfit strains in this film/substrate system were estimated to be $u_{m1} \approx -5.4 \times 10^{-4}$ and $u_{m2} \approx -8 \times 10^{-5}$.²³ Taking into account that these values fall into the stability range of the ca'' polarization state, we calculated the dielectric anisotropy of PST film to be $\epsilon_{22}/\epsilon_{11} \approx 1.4$. The predicted degree of anisotropy is in reasonable agreement with the measured value of $\epsilon_{22}/\epsilon_{11} \approx 1.25$.¹⁴

Thus, the thermodynamic theory explains the influence of strain anisotropy on the dielectric properties of ferroelectric films. It may be further extended to describe the electric-field dependence of the dielectric response, which is important for the application of ferroelectric films in tunable microwave devices.

The research described in this letter was made possible in part by Grant No. I/75965 from the Volkswagen-Stiftung, Germany.

¹C. M. Foster, G.-R. Bai, R. Csencsits, J. Vetrone, R. Jammy, L. A. Wills, E. Carr, and J. Amano, *J. Appl. Phys.* **81**, 2349 (1997).

²T. Tybell, C. H. Ahn, and J.-M. Triscone, *Appl. Phys. Lett.* **75**, 856 (1999).

³N. Yanase, K. Abe, N. Fukushima, and T. Kawakubo, *Jpn. J. Appl. Phys., Part 1* **38**, 5305 (1999).

⁴S. K. Streiffer, J. A. Eastman, D. D. Fong, C. Thompson, A. Munkholm, M. V. Ramana Murty, O. Auciello, G. R. Bai, and G. B. Stephenson, *Phys. Rev. Lett.* **89**, 067601 (2002).

⁵M. Okano, Y. Watanabe, and S.-W. Cheong, *Appl. Phys. Lett.* **82**, 1923 (2003).

⁶V. Nagarajan, S. Prasertchoung, T. Zhao, H. Zheng, J. Ouyang, R. Ramesh, W. Tian, X. Q. Pan, D. M. Kim, C. B. Eom, H. Kohlstedt, and R. Waser, *Appl. Phys. Lett.* **84**, 5225 (2004).

⁷N. A. Pertsev, A. G. Zembilgotov, and A. K. Tagantsev, *Phys. Rev. Lett.* **80**, 1988 (1998); *Ferroelectrics* **223**, 79 (1999).

⁸Y. Watanabe, *Phys. Rev. B* **57**, 789 (1998).

⁹A. L. Roytburd, S. P. Alpay, V. Nagarajan, C. S. Ganpule, S. Aggarwal, E. D. Williams, and R. Ramesh, *Phys. Rev. Lett.* **85**, 190 (2000).

¹⁰Y. L. Li, S. Y. Hu, Z. K. Liu, and L. Q. Chen, *Appl. Phys. Lett.* **78**, 3878 (2001).

¹¹N. A. Pertsev, V. G. Kukhar, H. Kohlstedt, and R. Waser, *Phys. Rev. B* **67**, 054107 (2003).

¹²J. Junquera and Ph. Ghosez, *Nature (London)* **422**, 506 (2003).

¹³O. Diégues, S. Tinte, A. Antons, C. Bungaro, J. B. Neaton, K. M. Rabe, and D. Vanderbilt, *Phys. Rev. B* **69**, 212101 (2004).

¹⁴Y. Lin, X. Chen, S. W. Liu, C. L. Chen, J.-S. Lee, Y. Li, Q. X. Jia, and A. Bhalla, *Appl. Phys. Lett.* **84**, 577 (2004).

¹⁵J. S. Speck and W. Pompe, *J. Appl. Phys.* **76**, 466 (1994).

¹⁶L. Lahoche, V. Lorman, S. B. Roshal, and J. M. Roelandt, *J. Appl. Phys.* **91**, 4973 (2002).

¹⁷Lattice parameters of a strained epitaxial film can be evaluated by the x-ray diffraction. If the epitaxial interface is commensurate, a_1 , a_2 , and γ become equal to the lattice parameters of the substrate in the crystallographic plane parallel to its surface. When dense arrays of misfit dislocations form at the interface, lattice parameters in the epitaxial layer tend to those of a free standing film.

¹⁸M. J. Haun, E. Furman, S. J. Jang, H. A. McKinstry, and L. E. Cross, *J. Appl. Phys.* **62**, 3331 (1987).

¹⁹Our results are also valid for epitaxial films grown on (110)-oriented cubic or orthorhombic substrates and other substrates that do not induce shear strains in the film plane.

²⁰A. G. Bogdanov and R. A. Khomutetskaya, *Izv. Acad. Nauk USSR* **21**, 433 (1957).

²¹N. A. Pertsev, A. K. Tagantsev, and N. Setter, *Phys. Rev. B* **61**, R825 (2000).

²²J. Meng, G. Zou, Y. Ma, X. Wang, and M. Zhao, *J. Phys.: Condens. Matter* **6**, 6549 (1994).

²³The misfit strains were calculated from the measured lattice parameters of the PST film, which are given in Ref. 14. The lattice constant $a_0 \approx 0.39$ 197 nm of the prototypic cubic cell was found by fitting the theoretical out-of-plane lattice parameter to the measured value.